ACS OMEGA

http://pubs.acs.org/journal/acsodf

Article

Adsorption Equilibrium and Diffusion of CH_4, CO_2, and N_2 in Coal-Based Activated Carbon

Bo Zhang,* Ping Liu, Zhuoran Huang, and Jingji Liu

Cite This: *ACS Omega* 2023, 8, 10303−10313

Read Online

ACCESS | Metrics & More | Article Recommendations

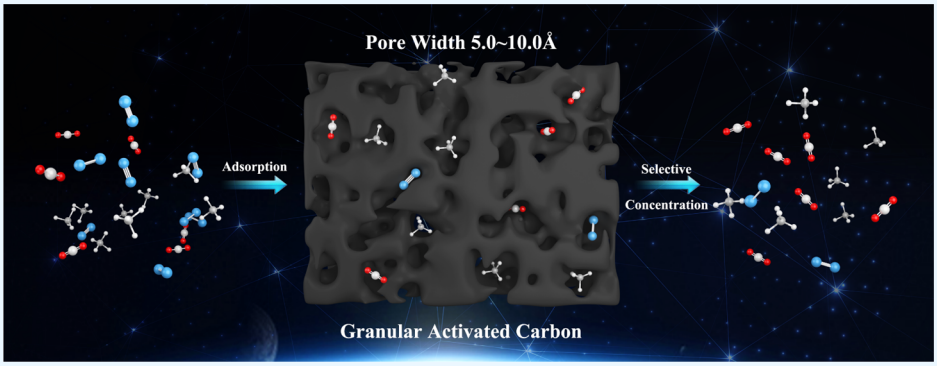

ABSTRACT: Coal-based activated carbon is an ideal adsorbent for concentrating CH_4 from coalbed methane and recovering CO_2 from industrial waste gas. In order to upgrade the environmentally protective preparation technology of coal-based activated carbons and clarify the adsorption equilibrium and diffusion rules of CH_4, CO_2, and N_2 in these materials, we prepared granular activated carbon (GAC) via air oxidation, carbonization, and physical activation using anthracite as the raw material. Also, we measured the adsorption isotherms and adsorption kinetic data of GAC by the gravimetric method and characterized its surface chemical properties. According to the results, GAC had abundant micropore structures with a pore size mainly in the range of 5.0−10.0 Å, and its surface was covered with plentiful oxygen-containing functional groups. The specific pore structure and surface chemical properties could effectively improve the separation and purification effects of GAC on CH_4 and CO_2. In the temperature range of 278−318 K, the equilibrium separation of CH_4/N_2 by GAC with a coefficient between 3 and 4 could be achieved. Also, the CO_2/CH_4 separation coefficient decreased with the increase in temperature but remained around 3. The bivariate Langmuir equation could describe the adsorption behaviors of GAC on CH_4/N_2, CO_2/N_2, and CH_4/CO_2. With the increase in the concentrations of CH_4 and CO_2 in the gas phase, the difference between the adsorption capacity of CH_4 or CO_2 and that of N_2 became greater. The change of the gas ratio did not affect the characteristics of preferential adsorption of CH_4 and CO_2. At different temperatures (278, 298, and 318 K), the diffusion coefficients of CH_4, N_2, and CO_2 at various pressure points showed predominately a small variation without an obvious trend. These results demonstrated that the separation of CH_4/N_2, CO_2/N_2, and CH_4/CO_2 by the activated carbon could only rely on the equilibrium separation effect rather than the kinetic effect.

1. INTRODUCTION

"Peaking carbon dioxide emissions and carbon neutrality" has been incorporated into China's overall strategic plan for ecological progress in order to implement green and low-carbon development. Methane (CH_4) is the main component of coal gas, natural gas, and shale gas and is also an important clean energy source. Besides, CH_4 is one of the greenhouse gases, and its greenhouse effect and destructive power to ozone layer are more than 20 times stronger than those of carbon dioxide (CO_2).[1] Generally, methane content should be greater than 90% to meet the requirements for pipeline transportation. The low-concentration coal mine gas usually has a small CH_4 content with many impurities and is often mixed with a large amount of air. Hence, concentrating methane from low-concentration coal mine gas via CH_4/N_2 separation is a reliable way to achieve the most greenhouse gas-intensive scenarios.[2] CO_2 is the main factor leading to the greenhouse effect, being also an important raw material for chemical synthesis. In addition, CO_2 plays an essential role in agriculture, petroleum exploitation, and shale and coal seam gas extraction.[3] The

Received: December 12, 2022
Accepted: March 1, 2023
Published: March 9, 2023

ACS Publications

© 2023 The Authors. Published by American Chemical Society

Table 1. Coal Composition Analysis Result of Chongqing Anthracite

proximate analysis (%)				Elemental analysis (%)				
fixed carbon	volatile components	ash content	moisture	C_{ad}	H_{ad}	O_{ad}	N_{ad}	S_{ad}
72.08	10.03	16.81	1.08	72.61	2.757	6.810	1.976	4.536

separation of CO_2/N_2 from flue gas has always been a hot topic in gas separation. Among various gas separation methods, pressure swing adsorption (PSA) is the most energy saving and cheapest technique. Previous studies have shown that PSA is an ideal tool for the separation of CH_4/N_2, CO_2/N_2, and CH_4/CO_2.[4] Although the PSA technology is relatively mature, the adsorbent used for gas separation has always been an important limiting factor affecting the separation effect of PSA.

Activated carbon is a kind of carbon adsorption material composed of microcrystalline carbon and amorphous carbon. Its most significant characteristics are large specific surface area and high adsorption capacity. The research on the preparation of activated carbon as well as the evaluation of CH_4 and CO_2 concentrations has never stopped. Twenty years ago, Lozano-Castelló et al.[5] prepared activated carbon powder with an extremely large specific surface area (up to 3290 m^2/g) and micropore volume (1.45 cm^3/g) by using anthracite as the raw material. Yacob et al.[6] produced activated carbon from waste wood, and its specific surface area could reach 1139 m^2/g. Buczek's research group[7] conducted a systematic experimental study on the applications of activated carbon to concentrate CH_4 in coal seam gas. The results showed that the large micropore volume of the adsorbent was not always conducive to the concentration of CH_4. Moreover, the separation effect of the adsorbent on CH_4 gradually decreased with the increase of the micropore volume, and the pore size was a very important factor affecting the separation effect. In addition, Brea used various kinds of activated carbon to study the penetration curve models of mixed gases such as CH_4, CO_2, N_2, and CO in the composite bed.[8] In recent years, nitrogen-doping technique for preparing activated carbon has attracted increasing attention from researchers. Govind from Canada[9] along with Park[10] and Lee[11] from South Korea prepared nitrogen-doped activated carbon and studied the influence of pore structure of activated carbon on CO_2 adsorption. In addition, Wang[12] from China prepared nitrogen-doped activated carbon with high adsorption capacity for CO_2. With the development of activated carbon preparation technologies, there are also some reports on the production of porous carbon materials using biomass waste.[13,14] It is noteworthy that though new-type zeolite molecular sieves have great potential in separating CH_4, CO_2, and N_2 mixtures,[15,16] activated carbon has elicited extensive research interest due to the capabilities for application in flue gas treatment, methane purification, adsorption and recovery of volatile organic compounds, prevention and control of air pollution, and so forth.[17−20] Among numerous studies, considerable attention has been paid to the effects of pore structure of activated carbon on CH_4 or CO_2 concentration.[21] The adsorption and diffusion of CH_4, CO_2, and N_2 in the micropore structure of activated carbon are thus worthy of further study and discussion.

Herein, granular activated carbon (GAC) was prepared from anthracite via air preoxidation, carbonization, and physical activation. First, the equilibrium separation and adsorption kinetics of CH_4/N_2, CO_2/N_2, and CH_4/CO_2 mixtures were studied through measuring the adsorption isotherms of CH_4, CO_2, and N_2 on GAC. Then, a thorough analysis of the pore structure and surface chemical properties of GAC at the microlevel was performed, and the factors affecting the concentration effect of GAC on CH_4 or CO_2 were discussed. According to the results, a stable and environmentally friendly preparation process of coal-based activated carbon could be mastered at the macrolevel, and efficient concentration of CH_4 and CO_2 could be achieved.

2. EXPERIMENTAL SECTION

2.1. Raw Materials and Preparation of Activated Carbon. The raw coal was the anthracite produced in Chongqing. The coal composition analysis results are shown in Table 1. The preparation process of GAC includes the following steps.

2.1.1. Pulverization of Raw Coal. First, the bulk raw coal was broken into small particles with a size less than 5 mm. Then, the raw coal was pulverized into a powder of about 160 mesh by using a sealed sample preparation pulverizer.

2.1.2. Preoxidation. The pulverized coal was placed in a muffle furnace and put in contact with air. The pulverized coal was heated to 300−450 °C at a constant heating rate and then kept for 1 h at the desired temperature. After being cooled to room temperature, the pulverized coal was taken out of the furnace.

2.1.3. Forming. Preoxidized coal powder and coal tar were weighed to be mixed in a proportion of 10:1. The coal tar was melted in an electric furnace and then mixed fully with the coal powder while adding a small amount of water. After that, the mixture was poured into a kneader and kneaded for 20−30 min. Finally, the mixture was poured into a forming machine to produce cylindrical particles with diameters of 3 mm and lengths of 3−5 mm.

2.1.4. Drying. The formed particles were put into a thermostatic drying oven and heated at 105 °C for more than 4 h to completely remove the moisture.

2.1.5. Carbonization. The dried samples were placed in a muffle furnace and heated to 500−700 °C at a rate of 5−10 °C/min under a N_2 atmosphere. The specimens were afterward kept at a constant temperature for a period of time to achieve full carbonization.

2.1.6. Activation. A flow of activator (water vapor or carbon dioxide) was put in a contact with the carbonized material to initiate the activation reaction at 800−950 °C. The flow was supplied for 1−3 h and then stopped.

After the muffle furnace was cooled down to room temperature, the samples were taken out and washed with water to remove impurities on their surface and then dried in the oven. Thus, the finished product of GAC was obtained.

2.2. Adsorption Isotherms. In this study, the adsorption isotherms of GAC were measured using an IGA-100B intelligent gravimetric analyzer produced by HIDEN Company, UK. Prior to the adsorption test, the adsorbent needs to be pretreated according to the following procedure. First, a certain mass of sample to be tested is loaded. Then, the balance chamber is sealed and connected to an external heating equipment. The sample is afterward heated for 10 h at 200 °C under vacuum. The purpose of this pretreatment is to

https://doi.org/10.1021/acsomega.2c07910
ACS Omega 2023, 8, 10303−10313

completely remove any impurities so that the adsorbent can exhibit its true adsorption properties. After pretreatment, the system temperature was set as the adsorption temperature, and the pressure points to be measured were determined. When the system temperature was stable, the adsorption isotherms and kinetic curves could be collected under pressures from vacuum to 2 MPa.

2.3. Pore Structure of Activated Carbon. An ASAP 2020M specific surface area and microstructure analyzer (Micromeritics, USA) was used to investigate the pore structure of the activated carbon. First, the samples were dried and desorbed at 150 °C for 6 h. Then, the adsorption isotherms at the relative pressure (P/P_0) of 10^{-6}−1 were measured under a N_2 atmosphere at the liquid nitrogen temperature (77 K). According to the adsorption isotherms, the specific surface area (S_{BET}), the micropore surface area (S_{mic}), the micropore size and volume (V_{mic}), the micropore size distribution, and the full pore distribution in the range of 0.4−300 nm were obtained by virtue of ASAP analysis software.

2.4. Surface Chemical Properties. The surface properties of activated carbon were qualitatively examined via Fourier transform infrared spectroscopy (FT-IR) using an infrared spectrometer (Nicolet MagnaIR550II, USA). X-ray photoelectron spectra (XPS) were obtained by an EDS7426 photoelectron spectroscope (Oxford, UK) to quantitatively analyze the surface composition of activated carbon.

2.5. Adsorption Equilibrium and Adsorption Selectivity. In order to distinguish between adsorbents with better separation performance for gas mixtures, a quick and simple calculation method needs to be established. In particular, it implies that the appropriate adsorbent parameters are easy to be estimated, can reflect the isothermal adsorption characteristics, and show the selectivity of adsorbents.

A trivial parametric theory consists in assuming that the adsorption isotherms of adsorbents meet the Langmuir law, that is, the coverage rate achieves its limit and the energy is uniformly distributed on the adsorbent surface when the saturation adsorption pressure is reached. In this respect, the Langmuir equation of a binary gas mixture is

$$q_i = (q_{mi} b_i p_i)/(1 + b_1 p_1 + b_2 p_2) \tag{1}$$

The equilibrium selectivity parameters can be defined as follows

$$\alpha_{1,2} = (x_1/x_2)/(y_1/y_2) \tag{2}$$

where x_1 and x_2 are the mole fractions of the two components in the adsorption phase; y_1 and y_2 are the mole fractions of the two components in the gas phase. Generally, it is considered that component 1 is the component that is easier to be adsorbed. By combining eq 2 and the binary Langmuir equation, it can be seen that the adsorption selectivity for component 1 is a constant over the whole adsorption pressure range

$$\alpha_{1,2} = (q_{m1} b_1)/(q_{m2} b_2) \tag{3}$$

The above method is afterward used in this study to calculate the equilibrium separation coefficients and to compare the selectivity of adsorbents.

2.6. Adsorption Kinetics—Diffusion Characteristics. In the field of gas separation, particular attention is paid to the research on practical applications of mass-transfer process. The diffusion coefficient is an important parameter in the mass transfer, which can characterize the diffusion and migration of the components in the system. Assume that the gas diffusion in crystals conforms to the Fickian laws. When the gas diffuses through the cross-section of a solid particle, the diffusion flux of each cross section in the medium is proportional to the product of concentration gradient and diffusion coefficient, and the concentration gradient is thus the driving force of the mass transfer. The concentration gradient is the driving force for the transfer, making the diffusion to take place in a single direction. Then, the diffusion equation can be expressed as[22]

$$D\left[\frac{\partial^2 C}{\partial r^2} + \frac{2}{r}\frac{\partial C}{\partial r}\right] = \frac{\partial C}{\partial t} \tag{4}$$

where D is the diffusion coefficient of gas in activated carbon, m^2/s; C is the concentration of the diffuser, mol/m^2; r is the radial coordinate; t is the time, s. The initial conditions and boundary conditions are

$$\begin{aligned} &r = 0, \quad \partial C/\partial r = 0 \\ &r = R, \quad C = C_0 \\ &t = 0, \quad C = 0 \end{aligned} \tag{5}$$

Using eq 5 to solve eq 4, it can be obtained

$$\frac{q_t}{q_\infty} = 1 - \frac{6}{\pi^2}\sum_{n=1}^{\infty}\frac{1}{n}\exp\left[-\frac{Dn^2\pi^2 t}{R^2}\right] \tag{6}$$

where q_t is the adsorption capacity at time t, q_∞ is the equilibrium adsorption capacity, n is a natural number, and R is the radius of the adsorbed particle. When $q_t/q_\infty > 40\%$, the values of t and $\ln(1-q_t/q_\infty)$ can be fitted to obtain a linear relationship. For the fitted line, the slope is $K = \pi^2 D/R^2$, from which it can be obtained that $D = KR^2/\pi^2$.

The relationship between the diffusion coefficient and the temperature can be described by the Arrhenius equation as follows

$$D = D_0 \exp(-E_a/RT) \tag{7}$$

where D_0 is the pre-exponential factor of the diffusion coefficient, m^2/s; E_a is the diffusion activation energy, kJ/mol; T is the temperature, K; R is the universal gas constant.

2.7. Thermodynamics of Adsorption. Physical adsorption is an exothermic reaction, and the amount of work done by the adsorption field is the amount of heat release. According to the adsorption curve, the relevant parameters of the adsorption heat can be calculated by the Clausius−Clapeyron equation. When the adsorption amount is a, the calculation formula of the adsorption heat is as follows

$$\ln P = \frac{-Q(a)}{RT} + C \tag{8}$$

3. RESULTS AND DISCUSSION

3.1. Pore Structure of Activated Carbon. As can be seen from Figure 1 and Table 2, the prepared GAC has abundant micropores. Previous research has shown that the activated carbon with good separation performance always has a relatively large specific surface area. The specific surface area and pore volume of micropores play an important role in the separation performance of activated carbon, and the pore size distribution is a key factor affecting the separation performance

https://doi.org/10.1021/acsomega.2c07910
ACS Omega 2023, 8, 10303−10313

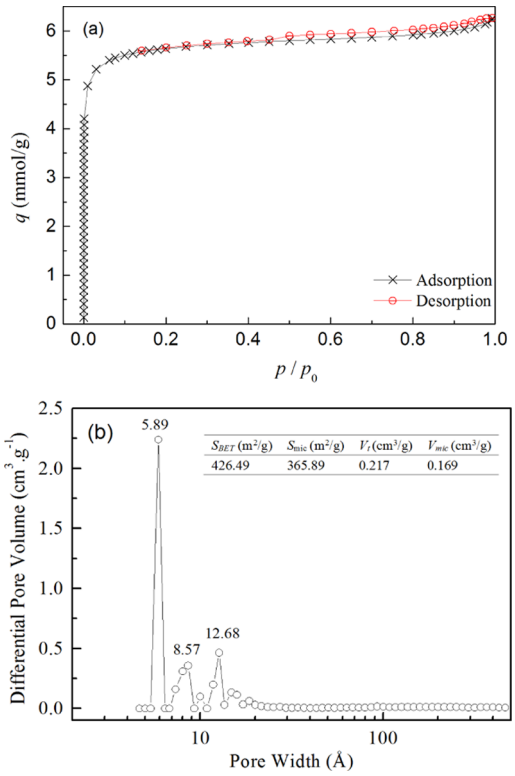

Figure 1. (a) Adsorption and desorption isotherms of nitrogen at 77 K and (b) pore size distribution of GAC.

Table 2. Pore Structure Parameters of GAC

pore size peak (Å)	pore size range corresponding to pore size peak (Å)	accumulated pore volume $V \times 10^3$ (cm^3/g)	accumulated surface area S (m^2/g)
5.89	5.36−6.43	88.66	300.68
8.57	6.79−9.29	27.61	68.34
12.68	9.29−17.16	34.38	53.73

of this material.[21] For example, in the separation of mixed gases, if the pore size of the adsorbents is just enough to allow N_2, but not CH_4 molecules, to enter, the separation of mixed gases can be achieved. In other words, the adsorption selectivity is closely related to the pore size. The research results of Kluson et al.[23] showed that the separation coefficient of the pores with the size less than 13 Å for CH_4/N_2 was above 3.0. Zhao et al.[24] considered that the pores with the size in the range of 0.758−0.776 nm had the best separation effect on CH_4/N_2, while Kluson et al.[23] believed that such a pore size should be 0.7−0.9 nm. The micropores of GAC are generally distributed in the size range of 5.0−10.0 Å, which is expected to ensure good separation performance.

3.2. Surface Chemical Properties of Activated Carbon. *3.2.1. FT-IR Spectral Analysis.* Figure 2 shows the FT-IR spectra of raw anthracite and activated carbon samples. The peak at 3440 cm^{-1} corresponds to the O−H stretching vibration, whereas that at 2925 cm^{-1} is attributed to the hydrogen absorption on the aliphatic hydrocarbon and cycloalkane groups. The band at 2852 cm^{-1} is caused by the addition of KBr to the sample, the signature at 1380 cm^{-1} is due to the bending vibration of methyl, and the line at about 1600 cm^{-1} corresponds to the stretching vibration of C═C double bonds in the aromatic ring. The peak in the range of

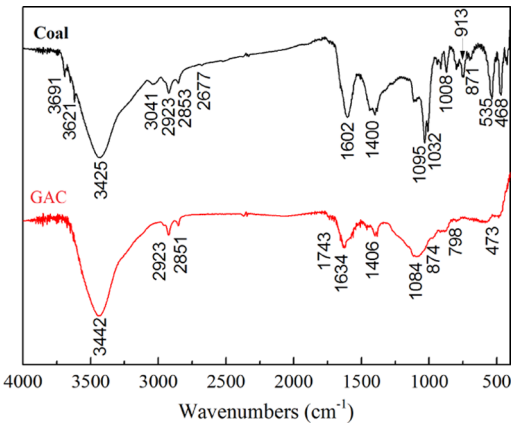

Figure 2. FT-IR spectra of anthracite coal and GAC.

1070−1090 cm^{-1} is attributed to the C−O stretching vibration, whereas that at 1040−910 cm^{-1} can be ascribed to the mineral or ash and the band at 753−743 cm^{-1} corresponds to the planar vibration of substituted aromatic hydrocarbons or methylene. The major structure of GAC is composed of multiple aromatic rings that are also connected to methyl, methylene, and oxygen-containing functional groups such as carboxyl and hydroxyl. Compared with anthracite, the absorption peak of GAC at 1100 cm^{-1} broadens obviously, indicating that there may be more oxygen-containing functional groups dominated by C−O bonds in each sample. This is because the preoxidation process increases the content of oxygen-containing functional groups on the surface of GAC. The carbonization process induces the polycondensation reaction of raw coal, which increases the content of highly substituted aromatic rings and removes the ash from the coal. The inlet of the activated gas can break the chemical bonds connecting the carbon network, causing the change of surface functional groups again.

3.2.2. XPS Spectra Analysis. By XPS tests, the categories and contents of functional groups on the GAC surface were quantitatively analyzed. Figure 3 displays the XPS peak split of GAC, and the fitting results are shown in Table 3.

It can be seen from Table 3 that the atomic mass fractions of C and O on the GAC surface are 90.4% and 9.6%, respectively. This proves quantitatively that GAC comprises many oxygen-containing functional groups such as C−O, C═O, and −COO−, among which the content of C−O functional groups is predominant. These results are consistent with the FT-IR

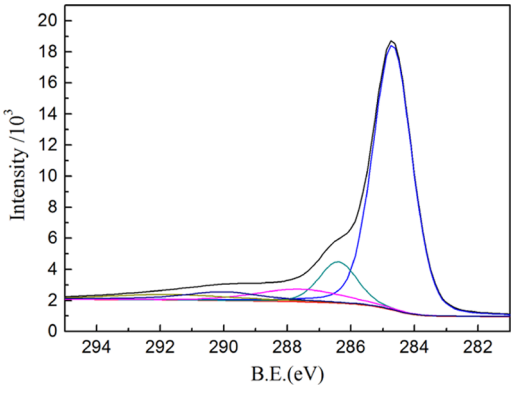

Figure 3. XPS peak split of GAC.

https://doi.org/10.1021/acsomega.2c07910
ACS Omega 2023, 8, 10303−10313

Table 3. XPS Peak Splitting Results on GAC

peak splitting	binding energy (eV)	area (cts-eV/s)	percentage (%)
Graphite-like carbon	284.7	28623	70.22
C−O	286.4	4366	10.71
C═O,O−C−O	287.6	3052	7.49
−COO−	290.0	2336	5.73
Carbon $\pi-\pi^*$ transition	291.7	2387	5.86
C_{1s}		34446	90.4
O_{1s}		28303	9.6

data. The categories of oxygen-containing functional groups on the surface of activated carbon can exhibit the adsorption selectivity to gas molecules with different polarities.[25,26] Although N_2, CH_4, and CO_2 are nonpolar molecules, both the C−H bonds in CH_4 and the C═O bonds in CO_2 are polar, and the polarizability of CH_4 or CO_2 is greater than that of N_2. Hence, the oxygen-containing functional groups on the surface of activated carbon are more likely to interact with CH_4 and CO_2 with higher polarizability. As a result, the adsorption capacity of GAC for CH_4 and CO_2 gets stronger, thus increasing the difference between the adsorption capacity of CH_4 or CO_2 and that of N_2, which is conducive to the equilibrium separation of CH_4/N_2 or CO_2/N_2. Some studies[27] have also shown that the oxygen-containing functional groups on the surface of activated carbon are conducive to the separation of CH_4/N_2. Therefore, the adsorption and separation performance of activated carbon can be improved by the combination of ideal micropore distribution and appropriate surface properties.

3.3. TGA/DTA Analysis. Figure 4 shows the thermogravimetric analysis (TGA)/differential thermal analysis (DTA)

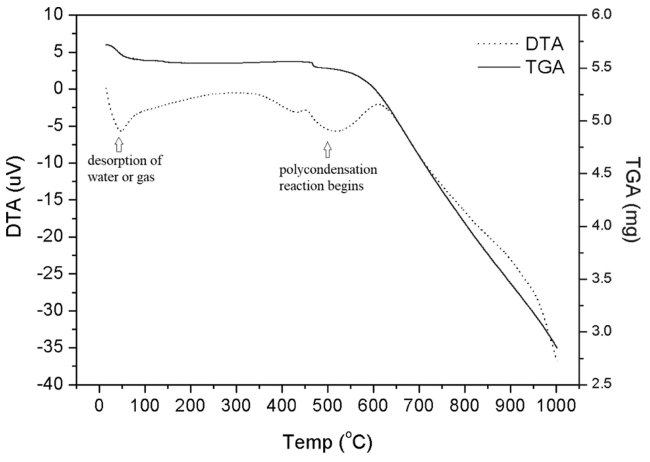

Figure 4. TGA-DTA curves of GAC.

curve of GAC, from which it can be seen that the sample mainly goes through the following three stages during pyrolysis.

(1) There is a faster weight loss peak between 0 °C and 70 °C, and the corresponding DTA curve shows an endothermic peak, which is mainly caused by the desorption of water or gas on the surface of activated carbon.
(2) When the temperature ranges from 70 °C to 460 °C, there is basically no change in thermogravimetric loss, indicating that most of the volatiles in the raw materials used for sample preparation have been removed during the preparation process.
(3) When the temperature is between 460 °C and 1000 °C, thermal weight loss starts to increase significantly, and when the temperature is around 520 °C, the DTA curve shows an obvious endothermic peak, which indicates that with the increase of temperature, the polycondensation reaction begins, excessive polycondensation occurs in the carbon skeleton of the sample, the pores begin to shrink and close, and some micropores gradually become mesoporous or macroporous or even collapse leading to mass reduction.

It can be seen that the prepared activated carbon sample has good thermal stability below 400 °C. When the ambient temperature is higher than 400 °C, its structure may be damaged and lose the adsorption property.

3.4. Adsorption Selectivity. The adsorption isotherms of CH_4, N_2, and CO_2 on the activated carbon were measured at 278, 298, and 318 K, respectively, and are shown in Figure 5.

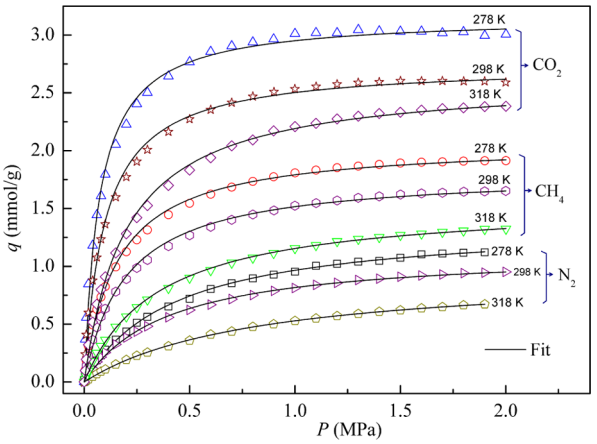

Figure 5. Adsorption isotherms of GAC-activated carbon for CH_4, N_2, and CO_2 at different temperatures.

As can be seen, the adsorption capacities of CH_4, N_2, and CO_2 follow the order of CO_2 > CH_4 > N_2, all decreasing with the increase of adsorption temperature under the same pressure.

Langmuir fitting was performed on the adsorption isotherms at these three temperatures, and the obtained fitting parameters are listed in Table 4.[28] As can be seen, q_m and b have the same variation rules, both decreasing with the increase in temperature. These indicate that the temperature can affect the slope of the adsorption isotherm at the initial period, making it drop with the increase of temperature. Thus, the equilibrium separation coefficient also changes accordingly. The separation coefficients at different temperatures are given in Table 5.[28]

According to previous studies, the adsorption selectivity coefficient (equilibrium separation coefficient) of CH_4/N_2 on activated carbon is mostly less than 5.0. For example, the equilibrium separation coefficient of K01 activated carbon is between 2 and 5,[29] that of the modified activated carbon can be improved to 4.0,[30] and that of coconut shell-activated carbon for CH_4/N_2 can reach 4.21.[31] However, there are also some reports revealing high separation coefficients. For example, the separation coefficient of AX-21 super activated carbon is 20.13, whereas that of nut shell-activated carbon is

https://doi.org/10.1021/acsomega.2c07910
ACS Omega 2023, 8, 10303−10313

Table 4. Fitting Parameters for GAC Using the Langmuir Equation at Different Temperatures

	qm (mmol/g)			b (MPa^{-1})		
	278 K	298 K	318 K	278 K	298 K	318 K
N2	1.30	1.14	0.96	2.60	2.51	1.22
CH4	2.07	1.81	1.56	6.45	5.11	2.85
CO2	3.16	2.75	2.63	13.99	10.29	5.03

Table 5. Adsorption Selectivity Parameters of GAC for CH_4, N_2, and CO_2 at Different Temperatures

	$\alpha_{CH4,N2}$	$\alpha_{CO2,N2}$	$\alpha_{CO2,CH4}$
278 K	3.95	13.1	3.31
298 K	3.23	9.89	3.06
318 K	3.80	11.29	2.97

12.93.[32] Unfortunately, these activated carbons with high separation coefficients have not been applied in the PSA process. Ruan et al.[33] reported a separation coefficient of about 5−7 for CO_2/N_2 on activated carbon. According to Foeth et al.,[34] the calculated separation coefficient of activated carbon for CO_2/CH_4 was up to 3.5. However, larger adsorption selectivity coefficient is not always good for the separation of gas mixture. Jasra et al.[35] conducted an experimental study on the separation performance of activated carbon. By combining their results with the research of Ruthven et al.,[36] they drew some conclusions as follows: when the separation coefficient was less than 2, it was difficult to separate the gas mixture; at the separation coefficient between 2 and 3, the separation of the gas mixture could be achieved; if the separation coefficient was greater than 3, the separation process was economical, whereas it made no significant sense when the separation coefficient was above 4. Thus, the appropriate separation coefficient should be between 3 and 4.

As seen in Table 5, the separation coefficients of GAC for CH_4/N_2 at all three temperatures are between 3 and 4, indicating that GAC can perform the separation of CH_4/N_2 within this temperature range well. However, the separation coefficient for CH_4/N_2 exhibits no monotonic change with the increase in temperature. Instead, it has the lowest value at 298 K but is relatively higher at 278 and 318 K. The variation of the separation coefficient for CO_2/N_2 follows the same rules. In turn, the separation coefficient for CO_2/CH_4 slightly decreases with the increase in temperature. The separation coefficient

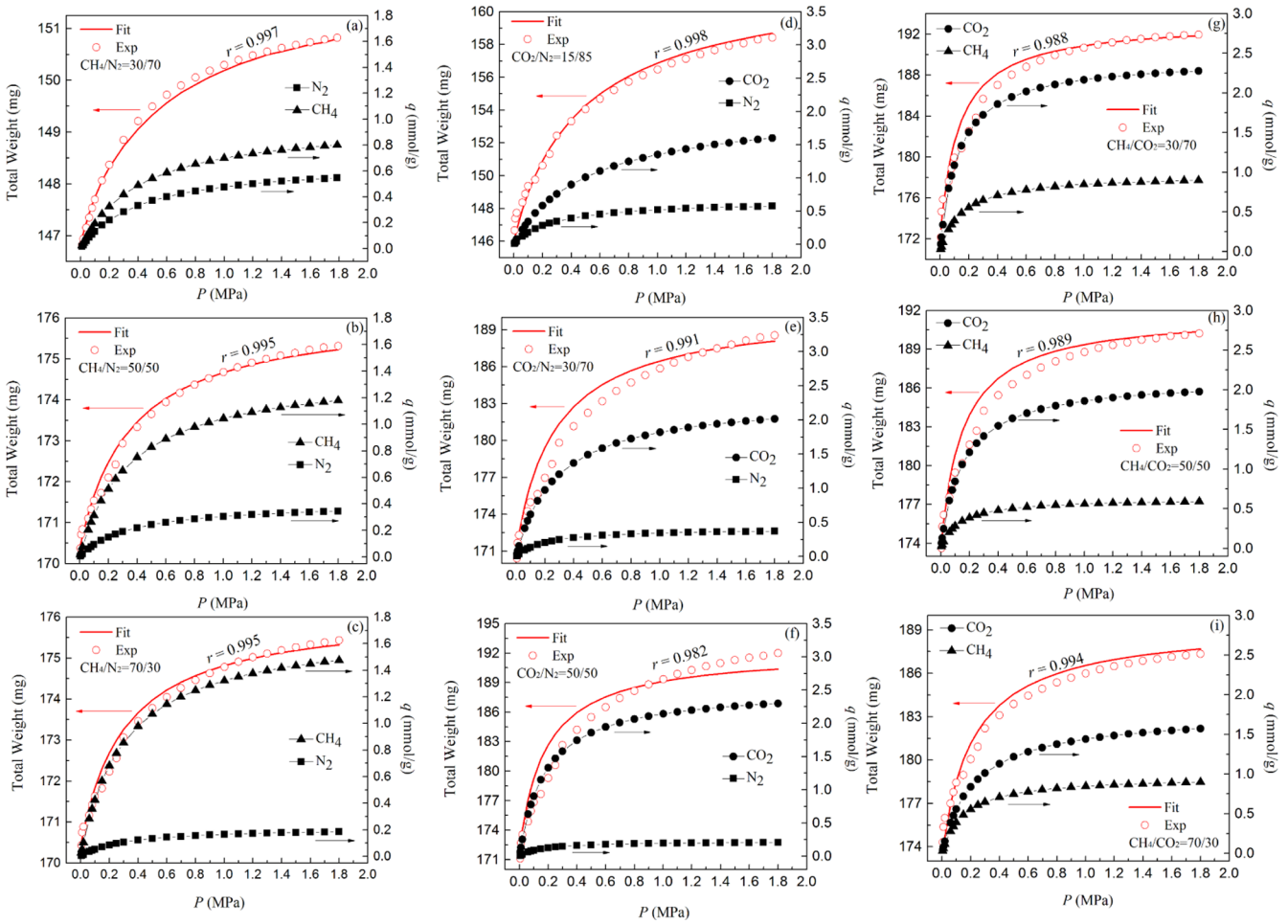

Figure 6. Adsorption isotherms of binary mixtures: experimental data and values calculated using Langmuir equation. (a−c) mixture of CH_4 and N_2; (d−f) mixture of CH_4 and N_2; (g−i) mixture of CO_2 and CH_4.

https://doi.org/10.1021/acsomega.2c07910
ACS Omega 2023, 8, 10303−10313

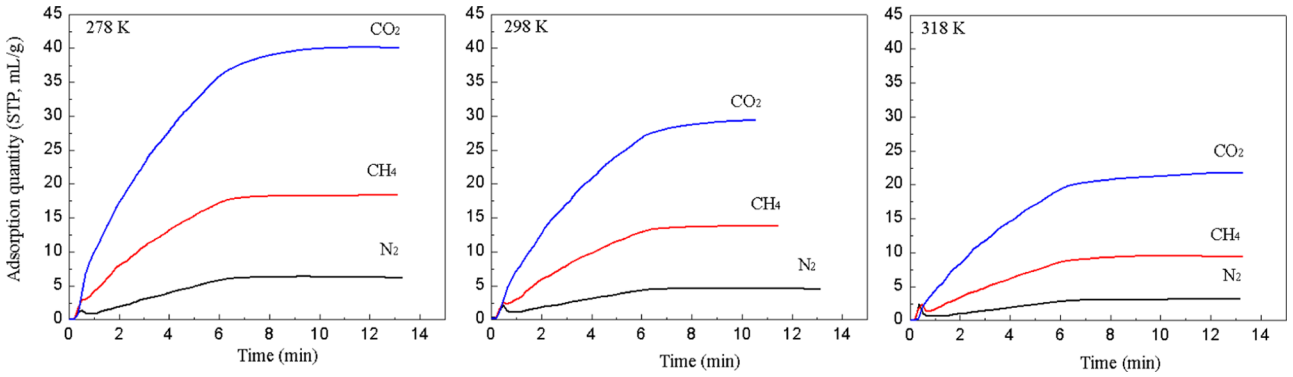

Figure 7. Kinetic curves for CH_4, N_2, and CO_2 at 278, 298, and 318 K.

values are all around 3, indicating that GAC can separate CO_2/CH_4 within this temperature range. Moreover, low temperature is more conducive to improving the separation effect.

3.5. Adsorption Isotherms of Binary Gas Mixture. Although single-component gas adsorption isotherms can be used to calculate the gas separation coefficients of binary gas mixtures, they fail to visually describe the actual situation of the mixed gas adsorption. This is because of the competitive adsorption and the interaction between different gas molecules. Hence, it is necessary to determine the adsorption isotherms of binary gas mixtures in order to further understand the adsorption situation of each component. Here, the adsorption isotherms of gas mixtures with different gas ratios at 298 K were tested, and the binary Langmuir equation (eq 1) was then used to calculate the partial adsorption capacity of each component. By establishing the correlation between calculated and experimental values, the accuracy of the calculation model can be evaluated. After calculating the partial adsorption capacity of each component by the proposed model, the partial adsorption capacity was converted into the gas mass. The gas mass plus the dry mass of the adsorbent after IGA pretreatment was the total mass of the adsorbed gas and adsorbent, which was also the "total weight" measured by IGA. By comparing the two values, the accuracy and feasibility of the selected calculation model can be assessed. In Figure 5, the *x*-axis denotes the adsorption pressure, the left *y*-axis is attributed to the total weight (the sum of the masses of adsorbed gas and adsorbent), and the right *y*-axis (Q) is referred to the partial adsorption capacity of each component. Here, the partial adsorption capacity can be obtained from the calculation model, and the total adsorption capacity (Fit) after conversion is afterward correlated with the experimental value (Exp).

As can be seen from Figure 6, the values calculated by Langmuir equation and the experimental points are ideally correlated, and the correlation coefficients r are all above 0.98, indicating that the binary Langmuir equation can well describe the adsorption behaviors of activated carbon on CH_4/N_2, CO_2/N_2, and CH_4/CO_2. Also, Figure 5 reveals that for the adsorption of CH_4, CO_2, and N_2 on activated carbon, CH_4 and CO_2 are always strong adsorption components. Even if the concentrations of CH_4 and CO_2 in the gas phase are lower, their adsorption capacity in the adsorption phase is still greater than that of N_2. With increasing concentrations of CH_4 and CO_2 in the gas phase, the difference between their adsorption capacities and that of N_2 will be greater. For CH_4/CO_2 adsorption, CO_2 is the strong adsorption component, and its adsorption capacity is always greater than that of CH_4. This indicates that in the separation process of CH_4/N_2 and CO_2/N_2, CH_4 and CO_2 can be preferentially adsorbed even if the ratio of raw gas is changed. For the separation of CH_4/CO_2, CO_2 would be concentrated as an easily adsorbed component. In addition, the higher the concentration of CH_4 or CO_2 in the raw gas, the greater are their adsorption capacities and the farther are those from that of N_2.

3.6. Adsorption Kinetic Analysis. The adsorption kinetics data on CH_4, N_2, and CO_2 at 278, 298, and 318 K were measured under a pressure of 0.1 MPa (Figure 7). The diffusion coefficient for each gas was calculated using eq 6, and then the relationship between the diffusion coefficient and the temperature was expressed by Arrhenius equation (eq 7). The calculation results on the related parameters are shown in Table 6.

Table 6. Diffusion Coefficients, Pre-exponential Factors, and Diffusion Activation Energies for CH_4, N_2, and CO_2 under 0.1 MPa

gas	temperature (K)	D (m^2/s)	D_0 (m^2/s)	E_a (kJ/mol)
CH_4	278	1.42×10^{-13}	1.20×10^{-11}	10.44
	298	1.59×10^{-13}		
	318	2.38×10^{-13}		
N_2	278	8.30×10^{-14}	1.86×10^{-11}	12.76
	298	9.53×10^{-14}		
	318	1.54×10^{-13}		
CO_2	278	3.47×10^{-14}	6.01×10^{-11}	17.22
	298	5.78×10^{-14}		
	318	8.90×10^{-14}		

According to Table 6, the diffusion coefficients of CH_4, N_2, and CO_2 under 0.1 MPa have the same variation rules, and their D values follow the order of $CH_4 > N_2 > CO_2$ at each temperature. The diffusion activation energies of CH_4, N_2, and CO_2 on the inner surface of GAC are 10.44, 12.76, and 17.22 kJ/mol, respectively. These indicate that in the mass transfer process, CH_4 is first to diffuse into the pores of activated carbon, followed by N_2 and CO_2. Obviously, the diffusion coefficient of CH_4 is higher than those of N_2 and CO_2, which is consistent with the conclusions of other researchers.[22,37] In addition, for the same gas under 0.1 MPa, its diffusion coefficient increases with the increase of temperature, which indicates that a temperature rise increases the energy of gas molecules and makes them more active, thus accelerating the diffusion rate in the activated carbon.

Figure 8 displays the variations of the diffusion coefficients of CH_4, N_2, and CO_2 with the change of pressure at different

https://doi.org/10.1021/acsomega.2c07910
ACS Omega 2023, 8, 10303−10313

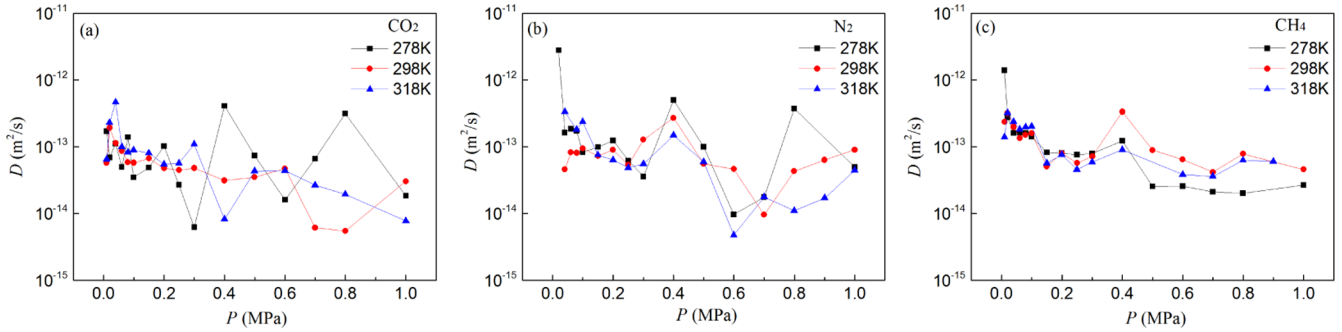

Figure 8. Diffusion coefficients with the change of pressure for (a) CO_2, (b) N_2, and (c) CH_4 at 278, 298, and 318 K.

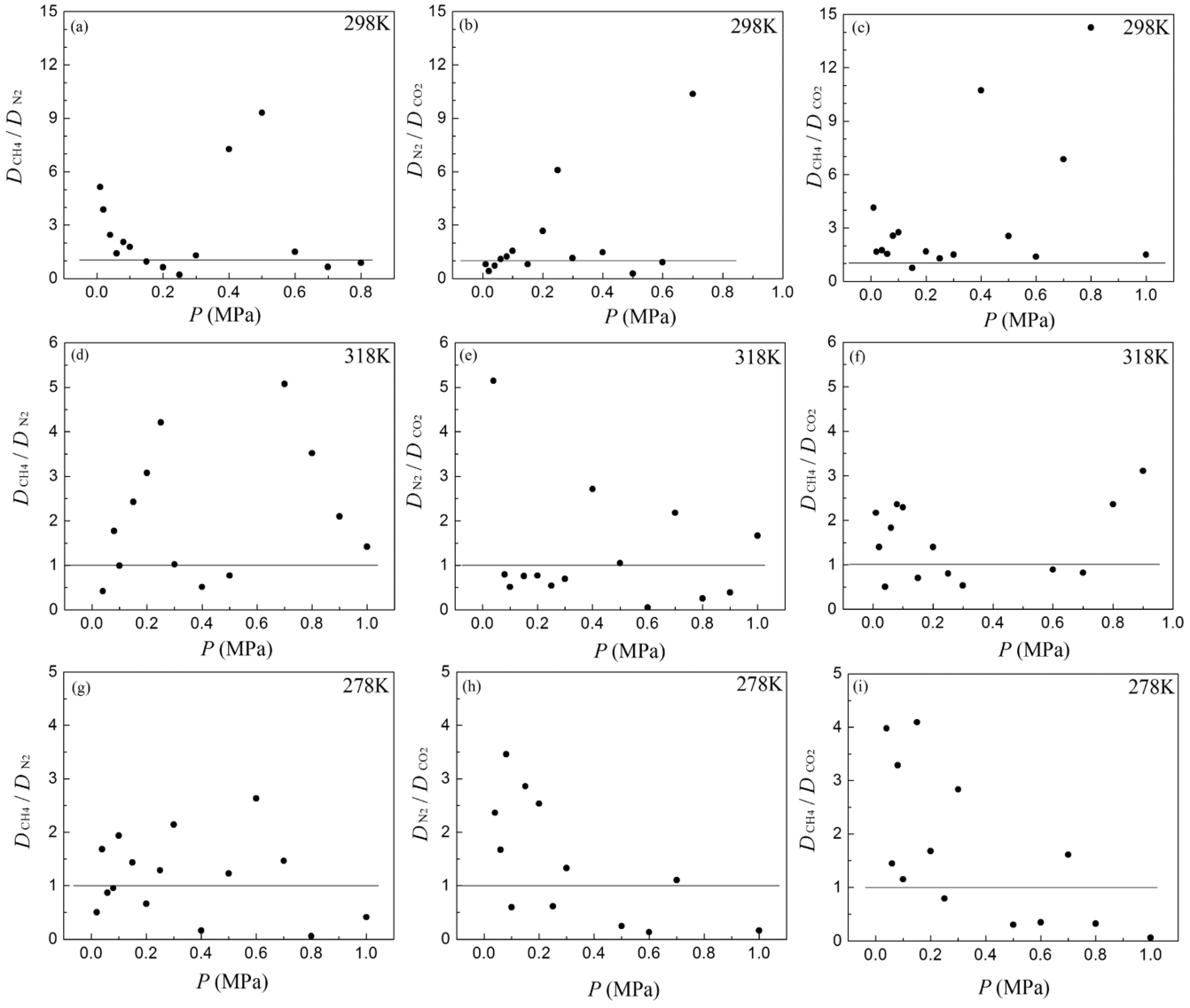

Figure 9. Diffusion coefficient ratios of gases on GAC at different temperatures. (a) D of CH_4/N_2 at 298 K, (b) D of N_2/CO_2 at 298 K, (c) D of CH_4/CO_2 at 298 K, (d) D of CH_4/N_2 at 318 K, (e) D of N_2/CO_2 at 318 K, (f) D of CH_4/CO_2 at 318 K, (g) D of CH_4/N_2 at 278 K, (h) D of N_2/CO_2 at 278 K, and (i) D of CH_4/CO_2 at 278 K.

temperatures. As can be seen, under the combined influences of pressure and temperature, the diffusion process is extremely complex. The diffusion coefficients exhibit no particularly evident variation rules but are mostly concentrated in a range of 10^{-12}–10^{-14} orders of magnitude. The general variation trend of the diffusion coefficient is to decrease with the increase of pressure. This is because the increase in pressure can lead to the increase in the adsorption capacity of the gas. As a result, the interaction between the gas molecules is enhanced, which induces the increase in the diffusion resistance of the adsorbent molecules in the adsorbent channels. The diffusion coefficient D of CH_4 fluctuates more

https://doi.org/10.1021/acsomega.2c07910
ACS Omega 2023, 8, 10303−10313

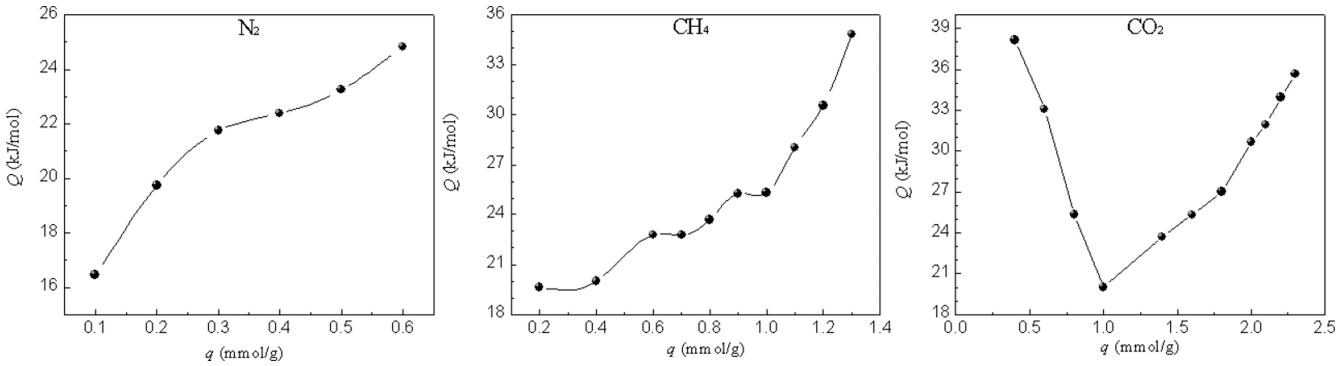

Figure 10. Adsorption heat with the change of the adsorption quantity for CH_4, N_2, and CO_2 on GAC.

slightly than those of N_2 or CO_2, which vary in an unsystematic manner. These differences are due to the fact that CH_4 molecules have a spherical shape, while N_2 and CO_2 molecules are rodlike. When the kinetic diameter of gas molecules is close to the adsorbent pore diameter, the shapes of molecules in the pores are random. In this respect, spherical molecules suffer from the least resistance and can enter the pores more smoothly. By contrast, rodlike or disklike molecules may be limited by the pore structure and shape and undergo a larger applied force or even resistance, thus complicating the diffusion process. This also proves from another aspect that the activated carbon sample may have many micropores close to molecular size.

Figure 9 displays the values of D_{CH4}/D_{N2}, D_{N2}/D_{CO2}, and D_{CH4}/D_{CO2} at different pressure points at 278, 298, and 318 K. According to Figure 7, the multiple differences in the diffusion coefficients of various gases can be directly obtained. The diffusion coefficient ratios have been widely used in the dynamic separation of gases by molecular sieves. Some researchers have found that the value of D_{N2}/D_{CH4} of 4A zeolite molecular sieve is between 9 and 18 in the temperature range of 273−313 K, which makes it possible to achieve the kinetic separation of PSA.[38] Qiu et al.[39] and Shi et al.[40] measured and calculated the diffusion coefficients of O_2 and N_2 on the carbon molecular sieve, and the value of D_{O2}/D_{N2} ranged from 5 to 10. It is noteworthy that the kinetic separation of PSA can be achieved when the ratio of the diffusion coefficients of two gases is close to 10[28]. As seen in Figure 8, there is a little difference in the diffusion coefficients of CH_4, N_2, and CO_2. While there are a few data points with a difference of more than 10 times in the diffusion coefficients, the values of D_{CH4}/D_{N2}, D_{N2}/D_{CO2}, and D_{CH4}/D_{CO2} at various pressures and different temperatures show no obvious change rules. These results demonstrate that the separation of CH_4/N_2, CO_2/N_2, and CH_4/CO_2 by GAC cannot resort to the kinetic effect.

3.7. Heat of Adsorption. Physical adsorption is an exothermic reaction. The heat released reflects the amount of work done by the adsorption field on the adsorbent surface. According to the adsorption data at 278, 298, and 318 K tested in Figure 5, the equal adsorption heat of N_2, CH_4, and CO_2 on GAC can be calculated by eq 8.

As can be seen from Figure 10, the adsorption heat of N_2, CH_4, and CO_2 on GAC is all less than 40 kJ/mol, which conforms to the law of physical adsorption. The adsorption heat of N_2 and CH_4 increases with the increase of adsorption amount, indicating that the intermolecular effect of gas is gradually increased during the whole adsorption process, and the change of adsorption heat of CH_4 has stepped fluctuations. This phenomenon is reflected in the adsorption of organic gas by zeolite because molecular rearrangement occurs on the adsorption surface, but the adsorption curve of CH_4 on activated carbon is type I. Gas molecules are a pure diffusion process without molecular rearrangement, so the adsorption heat change ladder of CH_4 may be caused by the uneven increase of the interaction between gas molecules. The adsorption heat of CO_2 decreases first and then increases. This phenomenon also occurs in the adsorption of methane by activated carbon because gas molecules preferentially occupy the adsorption sites with higher energy, and the adsorption heat decreases with the increase of adsorption capacity. When the gas molecules on the adsorption surface reach a certain concentration, the interaction between adsorbents began to increase and the adsorption heat began to increase with the increase of adsorption capacity.

4. CONCLUSIONS

The prepared activated carbon had a microporous structure with the pore sizes mainly distributed in the range of 5.0−10.0 Å, as well as a lot of oxygen-containing functional groups on its surface. In the temperature range of 278−318 K, the separation coefficient of CH_4/N_2 was between 3 and 4, which meant a desirable equilibrium separation of CH_4/N_2. The separation coefficient of CO_2/CH_4 decreased with the increase in temperature, remaining at around 3, which indicated that the equilibrium separation of CO_2/CH_4 could be achieved in this temperature range. A binary Langmuir equation could well describe the adsorption behaviors of CH_4/N_2, CO_2/N_2, and CH_4/CO_2 on activated carbon. Even if the concentrations of CH_4 and CO_2 in the gas phase were low, the adsorption capacity of CH_4 or CO_2 in the adsorption phase was still greater than that of N_2. With the increase in the concentrations of CH_4 and CO_2 in the gas phase, the difference between their adsorption capacity and that of N_2 would be greater. The results of adsorption kinetics showed that there was a little difference in the diffusion coefficients of CH_4, N_2, and CO_2. There were a few data points with a difference of more than 10 times in the diffusion coefficients, and the diffusion coefficients had no obvious change rules.

The specific pore structure and surface chemical properties of the activated carbon could effectively improve the separation and purification effects on CH_4 and CO_2. Although the specific surface area and pore volume of micropores played an important role in GAC's separation performance, the pore size distribution was found to be the decisive factor. The separation of CH_4/N_2, CO_2/N_2, and CH_4/CO_2 by the

https://doi.org/10.1021/acsomega.2c07910
ACS Omega 2023, 8, 10303−10313

activated carbon could rely on the equilibrium separation effect rather than on the kinetic effect.

AUTHOR INFORMATION

Corresponding Author

Bo Zhang − *College of Safety Engineering, Chongqing University of Science and Technology, Chongqing 401331, PR China*; orcid.org/0000-0001-7989-0568; Phone: +86 23 65023099; Email: zhangbo@cqust.edu.cn

Authors

Ping Liu − *College of Safety Engineering, Chongqing University of Science and Technology, Chongqing 401331, PR China*

Zhuoran Huang − *College of Safety Engineering, Chongqing University of Science and Technology, Chongqing 401331, PR China*

Jingji Liu − *Hangzhou Dianrun Chemical Co., LTD, Hangzhou 311200, PR China*

Complete contact information is available at: https://pubs.acs.org/10.1021/acsomega.2c07910

Notes

The authors declare no competing financial interest.

ACKNOWLEDGMENTS

This work was supported by the Scientific and Technological Research Program of Chongqing Municipal Education Commission (grant no. KJQN201901516).

REFERENCES

(1) Fan, Y.; Deng, C.; Zhang, X.; Li, F.; Wang, X.; Qiao, L. Numerical study of CO_2-enhanced coalbed methane recovery. *Int. J. Greenh. Gas Control* **2018**, *76*, 12−23.

(2) Doong, S. J.; Yang, R. T. Bulk separation of multi-component gas mixtures by pressure swing adsorption: pore/surface diffusion and equilibrium models. *AIChE J.* **1986**, *32*, 397−410.

(3) Li, J.; Wang, Y.; Chen, Z.; Rahman, S. S. Insights into the Molecular Competitive Adsorption Mechanism of CH_4/CO_2 in a Kerogen Matrix in the Presence of Moisture, Salinity, and Ethane. *Langmuir* **2021**, *37*, 12732−12745.

(4) Gomes, V. G.; Yee, K. W. K. Pressure swing adsorption for carbon dioxide sequestration from exhaust gases. *Sep. Purif. Technol.* **2002**, *28*, 161−171.

(5) Lozano-Castelló, D.; Lillo-Ródenas, M. A.; Cazorla-Amorós, D.; Linares-Solano, A. Preparation of activated carbons from Spanish anthracite I. Activation by KOH. *Carbon* **2001**, *39*, 741−749.

(6) Yacob, A. R.; Swaidan, H. M. A. Phosphoric Acid Effect on Prepared Activated Carbon from Saudi Arabia's Date Frond Waste. *Appl. Mech. Mater.* **2012**, *110−116*, 2124−2130.

(7) Buczek, B. Development of texture of carbonaceous sorbent f or use in methane recovery from gaseous mixtures. *Zesz. Nauk. - Politech. Lodz., Inz. Chem. Procesowa* **2000**, *61*, 285−292.

(8) Brea, P.; Delgado, J. A.; Águeda, V. I.; Uguina, M. A. Modeling of breakthrough curves of N_2, CH_4, CO, CO_2 and a SMR type off-gas mixture on a fixed bed of BPL activated carbon. *Sep. Purif. Technol.* **2017**, *179*, 61−71.

(9) Sethia, G.; Sayari, A. Comprehensive study of ultra-microporous nitrogen-doped activated carbon for CO_2 capture. *Carbon* **2015**, *93*, 68−80.

(10) Rehman, A.; Heo, Y.; Nazir, G.; Park, S. Solvent-free, one-pot synthesis of nitrogen-tailored alkali-activated microporous carbons with an efficient CO_2 adsorption. *Carbon* **2021**, *172*, 71−82.

(11) Lee, M.; Park, M.; Kim, H.; Park, S. Effects of Microporosity and Surface Chemistry on Separation Performances of N-Containing Pitch-Based Activated Carbons for CO_2/N_2 Binary Mixture. *Sci. Rep.* **2016**, *6*, 23224.

(12) Wang, L.; Rao, L.; Xia, B.; Wang, L.; Yue, L.; Liang, Y.; DaCosta, H.; Hu, X. Highly efficient CO_2 adsorption by nitrogen-doped porous carbons synthesized with low-temperature sodium amide activation. *Carbon* **2018**, *130*, 31−40.

(13) Wang, Y.; Liu, Y.; Chen, Z.; Zhang, M.; Liu, B.; Xu, Z.; Yan, K. In situ growth of hydrophilic nickel-cobalt layered double hydroxides nanosheets on biomass waste-derived porous carbon for high-performance hybrid supercapacitors. *Green Chem.* **2022**, *3*, 55−63.

(14) Chen, Z.; Zhang, M.; Wang, Y.; Yang, Z.; Hu, D.; Tang, Y.; Yan, K. Controllable synthesis of nitrogen-doped porous carbon from metal-polluted miscanthus waste boosting for supercapacitors. *Green Energy Environ.* **2021**, *6*, 929−937.

(15) Ullah, R.; Ali H Salah Saad, A. H. S. S.; Aparicio, S.; Atilhan, S. Adsorption equilibrium studies of CO_2, CH_4 and N_2 on various modified zeolites at high pressures up to 200 bars. *Microporous Mesoporous Mater.* **2018**, *262*, 49−58.

(16) Vaezi, M. J.; Babaluo, A. A.; Maghsoudi, H. Separation of CO_2 and N_2 from CH_4 using modified DD3R zeolite membrane: A comparative study of synthesis procedures. *Chem. Eng. Res. Des.* **2018**, *134*, 347−358.

(17) Wang, K.; Pan, J.; Wang, E.; Hou, Q.; Yang, Y.; Wang, X. Potential impact of CO_2 injection into coal matrix in molecular terms. *Chem. Eng. J.* **2020**, *401*, 126071.

(18) Trinh, T. T.; van Erp, T. S.; Bedeaux, D.; Kjelstrup, S.; Grande, C. A. A procedure to find thermodynamic equilibrium constants for CO_2 and CH_4 adsorption on activated carbon. *Phys. Chem. Chem. Phys.* **2015**, *17*, 8223−8230.

(19) Arami-Niya, A.; Rufford, T. E.; Zhu, Z. Activated carbon monoliths with hierarchical pore structure from tar pitch and coal powder for the adsorption of CO_2, CH_4 and N_2. *Carbon* **2016**, *103*, 115−124.

(20) Rosas, J. M.; Ruiz-Rosas, R.; Rodríguez-Mirasol, J.; Cordero, T. Kinetic study of SO_2 removal over lignin-based activated carbon. *Chem. Eng. J.* **2017**, *307*, 707−721.

(21) Gu, M.; Zhang, B.; Qi, Z.; Liu, Z.; Duan, S.; Du, X.; Xian, X. Effects of pore structure of granular activated carbons on CH_4 enrichment from CH_4/N_2 by vacuum pressure swing adsorption. *Sep. Purif. Technol.* **2015**, *146*, 213−218.

(22) Wang, F.; Shao, X.; Wang, W. Measurements of diffusion coefficient s for methane and carbon dioxide in activated meso-carbon microbeads. *Chin. J. Chem. Eng.* **2006**, *57*, 1891−1896.

(23) Kluson, P.; Scaife, S.; Quirke, N. The design of microporous graphitic adsorbents for selective separation of gases. *Sep. Sci. Technol.* **2000**, *20*, 15−24.

(24) Zhao, G.; Bai, P.; Zhu, H.; Yan, R.; Liu, X.; Yan, Z. The modification of activated carbons and the pore structure effect on enrichment of coal-bed methane. *Asia-Pac. J. Chem. Eng.* **2008**, *3*, 284−291.

(25) Song, X.; Wang, L.; Gong, J.; Zhan, X.; Zeng, Y. Exploring a New Method to Study the Effects of Surface Functional Groups on Adsorption of CO_2 and CH_4 on Activated Carbons. *Langmuir* **2020**, *36*, 3862−3870.

(26) Li, J.; Pan, J.; Wang, X.; Wang, K.; Nie, S.; Gao, D. Potential effect of carbon dioxide injection on the functional groups of medium volatile bituminous coals analysed using in-situ diffuse reflectance Fourier-transform infrared spectroscopy. *Int. J. Coal Geol.* **2023**, *265*, 104169.

(27) Gu, M.; Liu, K.; Xian, X.; Feng, Y. Preparation of granular active carbon by anthracite coal and its performance for separation CH_4/N_2 by pressure swing adsorption. *Mater. Sci. Technol.* **2011**, *19*, 82−87.

(28) Zhang, B.; Huang, Z.; Liu, P.; Liu, J.; Gu, M. Influence of pore structure of granular activated carbon prepared from anthracite on the adsorption of CO_2, CH_4 and N_2. *Korean J. Chem. Eng.* **2022**, *39*, 724−735.

(29) Zhang, B.; Gu, M.; Xian, X.; Lin, W. Adsorption equilibrium and diffusion of CH_4, N_2 and CO_2 in coconut shell activated carbon. *J. China Coal Soc.* **2010**, *35*, 1341−1346.

(30) Baksh, M. S. A.; Yang, R. T.; Chung, D. D. L. Composite sorbents by chemical vapor deposition on activated carbon. *Carbon* **1989**, *27*, 931−934.
(31) Zhang, J.; Wang, P.; Li, X.; Li, L.; Che, Y.; Qu, S. Equilibrium adsorption and kinetic diffusion mechanism of CH_4/N_2 on coconut shell-based activated carbon. *J. China Coal Soc.* **2020**, *45*, 427−435.
(32) Zhou, L.; Guo, W.; Zhou, T. A Feasibility Study of Separating CH_4/N_2 by Adsorption. *Chin. J. Chem. Eng.* **2002**, *10*, 558−561.
(33) Ruan, H. Study on adsorption and separation of CO2/N2 mixture gas, Ph.D. thesis, University of Tian Jin China, 2000, pp 48−50.
(34) Foeth, F.; Andersson, M.; Bosch, H.; Aly, G.; Reith, T. Separation of Dilute CO2-CH4Mixtures by Adsorption on Activated Carbon. *Sep. Sci. Technol.* **1994**, *29*, 93−118.
(35) Nettem, V. C.; Jasra, R. V.; Bhat, S. G. T. Separation of gases by pressure swing adsorption. *Sep. Sci. Technol.* **1991**, *26*, 885−930.
(36) Ruthven, D. M. *Principles of Adsorption and Adsorption Processes*; John Wiley & Sons, Inc., 1984; pp 20−30.
(37) Prasetyo, I.; Do, D. D. Adsorption rate of methane and carbon dioxide on activated carbon by the semi-batch constant molar flow rate method. *Chem. Eng. Sci.* **1998**, *53*, 3459−3467.
(38) Nazmul, H.; Ruthven, D. M. Chromatographic study of sorption and diffusion in 4A zeolite. *J. Colloid Interface Sci.* **1986**, *112*, 154−163.
(39) Qiu, J.; Guo, S. Adsorption and diffusion of oxygen and nitrogen in carbon molecular sieve. *J. Chem. Eng. Chin. Univ.* **1992**, *6*, 219−223.
(40) Shi, X.; Zhang, Y.; Wang, J. Diffusion of O_2, N_2, CH_4 on carbon molecular sieve. *Acta Pet. Sin.* **1999**, *15*, 81−83.

https://doi.org/10.1021/acsomega.2c07910
ACS Omega 2023, 8, 10303−10313